Investigation on parametric representation of proportional and nonproportional multiaxial fatigue responses

J. Albinmousa
Mechanical Engineering Department, King Fahd University of Petroleum & Minerals, Dhahran 31261, Saudi Arabia
binmousa@kfupm.edu.sa

ABSTRACT. This study aims to investigate fatigue damage resulting from multiaxial fatigue, proportional and/or nonproportional, loading by analyzing stresses and strains over a full domain around a representative stress-strain element. Plain stress-strain transformation of multiaxial hysteresis was performed by varying orientation of plane for $0 \leq \varphi \leq 2\pi$. Parametric representations for both normal and shear stresses and strains were obtained by plotting them in polar figures. These figures show that depending on the applied loading stresses and strains represent definitive known parametric curves.
Parametric representation of fatigue damage parameter such as Fatemi-Socie suggests that fatigue damage shall be calculated as the sum of the damage values on all planes. The proposed technique has been shown to improve fatigue life prediction compared to that obtained from the critical plane method.

KEYWORDS. Critical plane; Fatigue damage; Multiaxial fatigue; Parametric representation.

INTRODUCTION

Fatigue cracks initiate and grow at certain planes, i.e., persistent slip bands (PSBs). This established fact can be clearly observed in deformed single crystals [1-3]. Fatigue damage is associated with crack formation and critical plane concept originated based on this observation. Critical plane concept is widely used as the basis for formulating fatigue damage models. Therefore, fatigue damage is calculated at specific planes that are usually experience maximum value of either normal or shear strain or stress [4-7]. In some models, the critical plane is defined as the plane at which the value of the damage parameter is maximum [8].
On smooth specimen level, critical planes models have been shown to provide reasonable fatigue life predictions for different testing scenarios that include mean stress or strain, constant and variable amplitude loading, proportional and nonproportional loading conditions as well as complex loading paths [9]. However, Socie et al. [10] conducted a comparative numerical analysis on multiaxial fatigue benchmark experiment performed on simple notched SAE shaft [11]. Five software packages were used to compute the fatigue lives for 75 bending-torsion notched shafts. Socie et al. [10] showed that cumulative probability distribution for in-phase loading test on smooth tubular specimen indicates that there is 99% chance for fatigue life to be predicted within a factor of 2. Conversely, there is 99% chance for fatigue life to be predicted within a factor of 10 when it comes to notched shaft. Socie et al. [10] emphasized on the consideration of complex geometries and loading conditions for evaluating fatigue models. On the other hand, it is often found that models that are based on completely different critical plane assumptions such as normal or shear still give very similar fatigue life predictions [9, 12, 13]. Such observation raises two important questions. First, what is the "critical" plane? The second question is: if two criteria are based on two different critical plane assumptions predict similar fatigue lives then which one of them is correct? These arguments suggest that further development is required to improve not only fatigue life but also fatigue crack path predictions.

This paper aims to investigate fatigue damage resulting from multiaxial, proportional and nonproportional, loading by analysing stresses and strains over a full domain of a representative stress-strain element. A new technique for evaluating strain based fatigue damage without consideration of a particular critical plane has been proposed.

MATERIALS AND EXPERIMENTS

The material used for this investigation is micro alloyed fine grained structural steel S460N (FeE460) tested by Hoffmeyer et al. [14]. Axial-torsional loading was applied on smooth thin-walled tubes specimens under strain controlled condition and room temperature. Two multiaxial loading paths are considered for parametric analysis: proportional and 90° out-of-phase loading. The monotonic and cyclic properties of S460N steel are listed in Table 1. Details of the proportional and nonproportional cyclic tests can be found in Table 2. This material was selected because of its symmetric cyclic behaviour as shown in Fig. 1.

Property		Property	
E (MPa)	208,500	c	-0.493
ν	0.3	K_s' (MPa)	599
$\sigma_{0.2\%}$ (MPa)	500	n_s'	0.169
K'(MPa)	1115	τ_f' (MPa)	463.2
n'	0.161	γ_f'	0.224
σ_f' (MPa)	969.6	b_s	-0.071
ε_f'	0.281	c_s	-0.422
b	-0.086		

Table 1: Monotonic and cyclic properties of S460N steel [14].

No.	Loading	ε_a (%)	γ_a(%)	σ_a(MPa)	τ_a(MPa)	N_f (Cycles)
Nr20	0° Phase	0.173	0.300	244.2	147.3	31,100
Nr26	90° Phase	0.231	0.400	391.5	230.9	6,570

Table 2: Summary of cyclic tests [14].

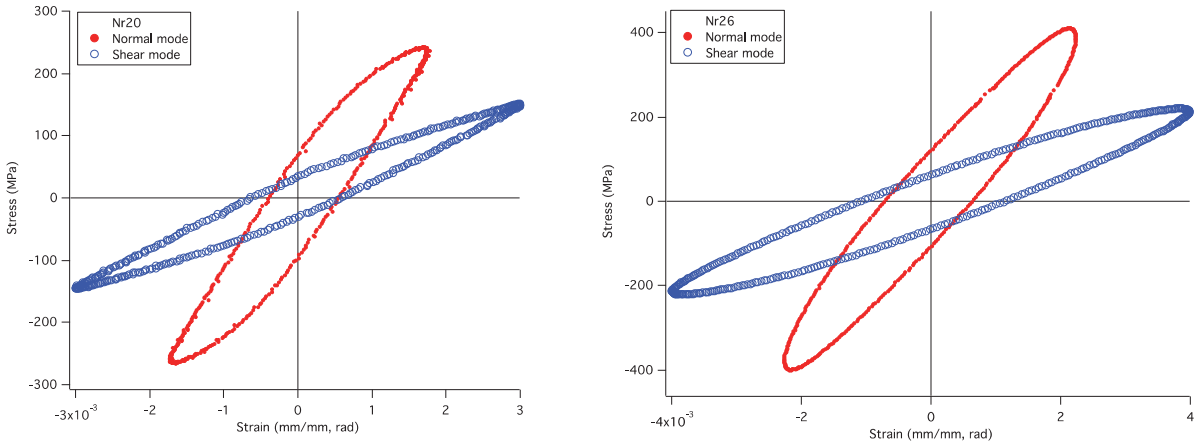

Figure 1: Axial-torsional hysteresis for proportional (Nr20) and nonproportional (Nr26) tests.

ANALYSIS AND MODELLING

Normal and shear cyclic responses in Fig. 1 were transformed using plane stress-strain transformation relations over the range $0 \leq \varphi \leq 2\pi$ with an increment of $\varphi_i = 1.0°$. Maximum stresses and strains at each angular increment were recorded and then plotted on polar diagrams. After that, each polar curve was fitted using proper parametric equation, Eqs. 1 to 8, as shown in Fig. 2 a to h, respectively.

$$\varepsilon_{max}(\varphi) = 0.00135 \sin^8\left(\varphi - \frac{\pi}{3}\right) \pm 0.00243 \cos^5\left(\varphi - \frac{\pi}{3}\right) \tag{1}$$

$$\sigma_{max}(\varphi) = \pm 70 \sin^{11}\left(\varphi - \frac{\pi}{3}\right) \pm 305 \cos^3\left(\varphi - \frac{\pi}{3}\right) \tag{2}$$

$$\gamma_{max}(\varphi) = 0.0018 \sin\left(4\varphi + \frac{\pi}{20}\right) + 0.00198 \tag{3}$$

$$\tau_{max}(\varphi) = 280 \sin\left(4\varphi + \frac{\pi}{14}\right) + 110 \tag{4}$$

$$\varepsilon_{max}(\varphi) = \frac{1}{450}(0.004 + \sin^2\varphi)^{0.2} \tag{5}$$

$$\sigma_{max}(\varphi) = 290(1 - \cos 2\varphi)^{0.5} \tag{6}$$

$$\gamma_{max}(\varphi) = \frac{1}{1000}(0.5 \cos 4\varphi + 3.5) \tag{7}$$

$$\tau_{max}(\varphi) = 212 + 10 \cos 4\varphi \tag{8}$$

It should be noted here that the plus and minus signs in Eqs. 1 and 2 represents two different equations for the top and bottom parts of the curves in Figs. 2a and b, respectively. Similar to the stress and strain responses, fatigue damage parameter can also be represented in a parametric form. Figure 3 shows the parametric representation of the Fatemi-Socie [5] fatigue damage parameter for the proportional, Nr20, and nonproportional, Nr26, loading cases. Hence, the Fatemi-Socie damage parameter was expressed in a parametric form as in Eq. 9.

$$D(\varphi) = \gamma(\varphi)\left(1 + k\frac{\sigma(\varphi)}{S_y}\right) \tag{9}$$

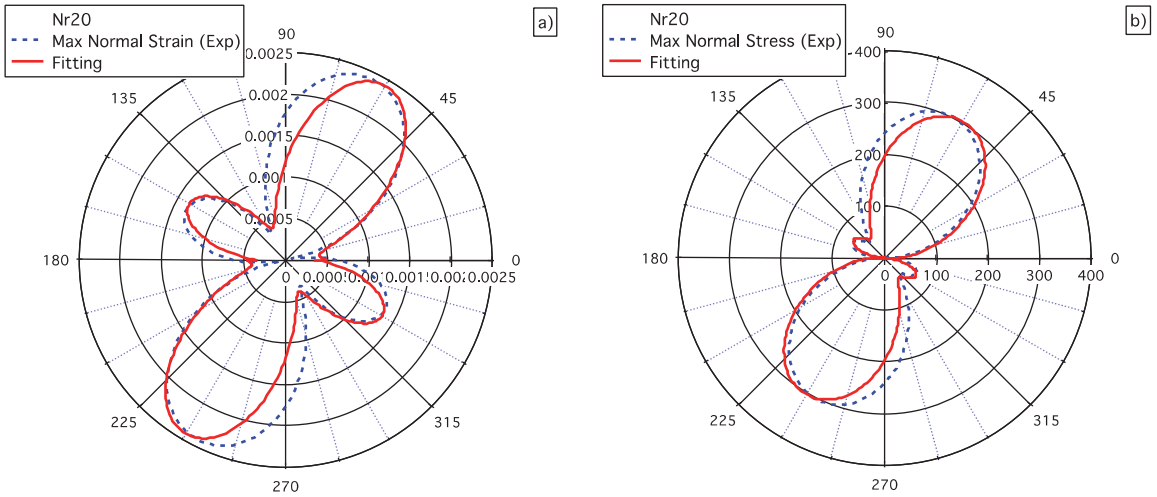

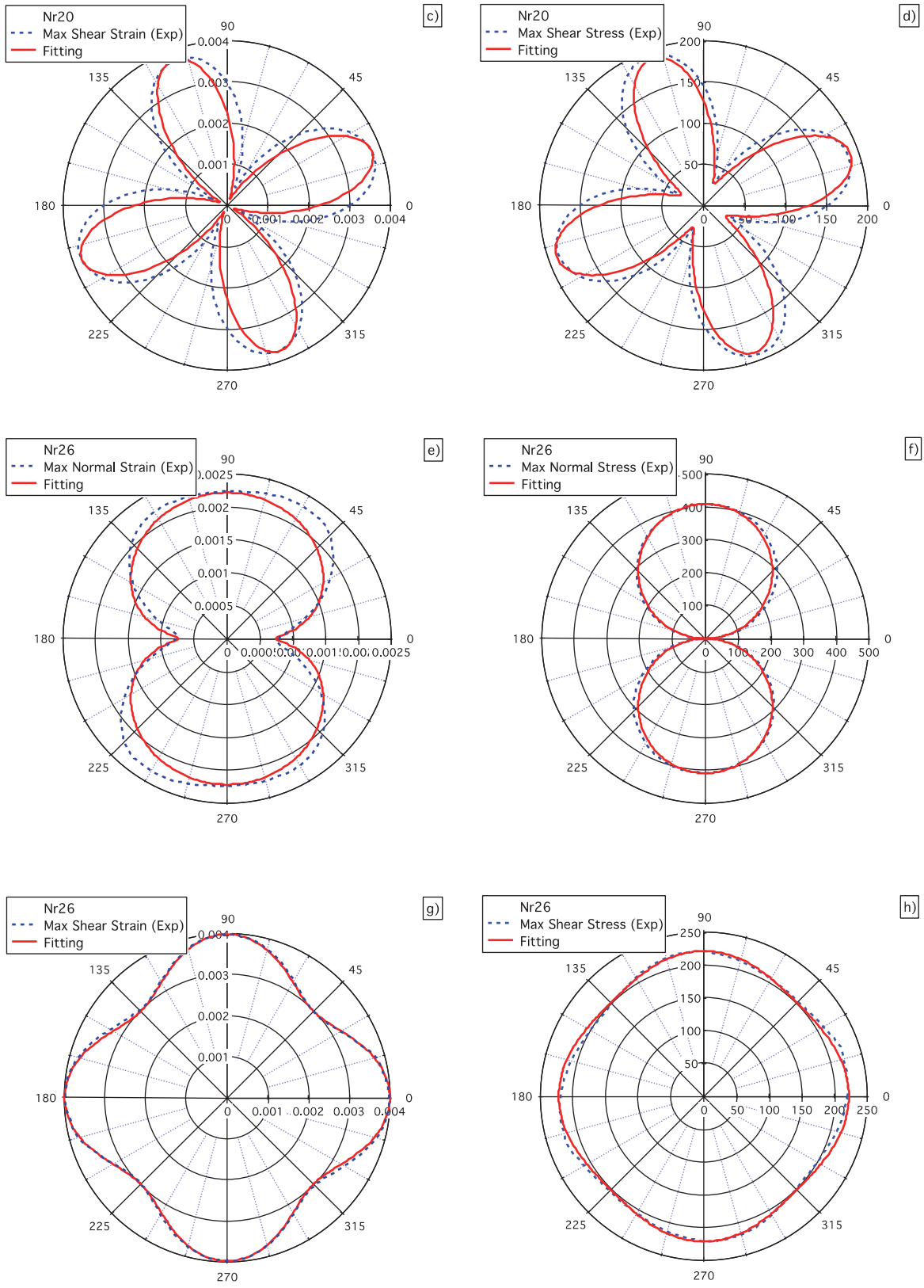

Figure 2: Parametric representation and fitting of the stress and strain responses for the proportional and nonproportional loading cases Nr20 and Nr26.

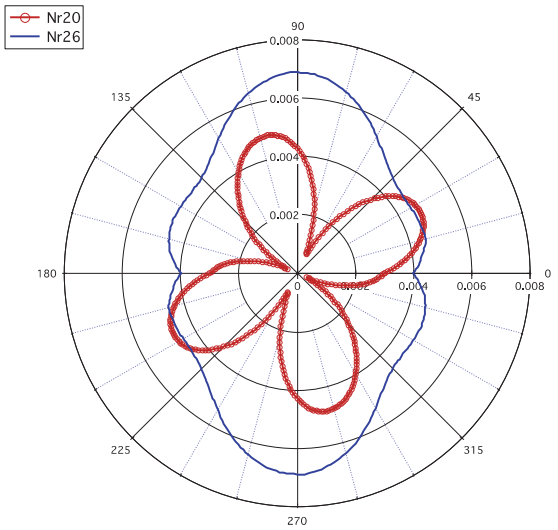

Figure 3: Parametric representation of Fatemi-Socie fatigue damage parameter for Nr20 and Nr26.

Discussion

Two observations can be made from the parametric modelling of the cyclic responses and the fatigue damage. First, stress and strain responses represent definitive known parametric curves. Further study is needed to investigate the possibility of formulating mathematical fatigue damage, fatigue life and fatigue crack path using parametric equations. Second, the polar diagram of the Fatemi-Socie parameter, Fig. 3, shows that substantial number of planes experience high damage. This observation was reported by Jiang et al [15]. It is proposed here that fatigue damage shall be calculated as the sum of all incremental damage on each plane as expressed in Eq. 10.

$$D = \sum_{\varphi=0}^{\varphi=2\pi} D(\varphi) = \sum_{\varphi=0}^{\varphi=2\pi} \gamma(\varphi)\left(1 + k\frac{\sigma(\varphi)}{S_y}\right) \tag{10}$$

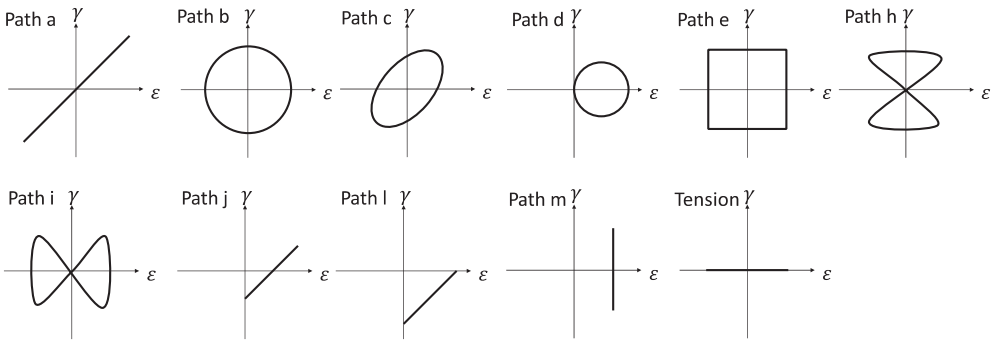

Figure 4: Parametric representation of Fatemi-Socie fatigue damage parameter for Nr20 and Nr26.

To verify this proposal, additional multiaxial fatigue data from Hoffmeyer et al. [14] were considered. These include tests from the eleven cyclic loading paths shown in Fig. 4. Fatigue damage and fatigue lives were correlated in Fig. 5a. These data were then fitted with a power relation as expressed in Eq. 11.

$$D = \kappa + \beta N_f^{\alpha} \tag{11}$$

where $\varkappa$ =0.311, β =26.01 and a =-0.329.
The predictions of Eq. 11 are compared with the experimental fatigue lives in Fig. 5b. In addition, the predictions of fatigue lives using standard Fatemi-Socie fatigue life model are also included in Fig. 5b. It can be seen from Fig. 5b that fatigue lives obtained by the proposed damage calculation method are mostly within $\pm$ 1.5x factor of lives.

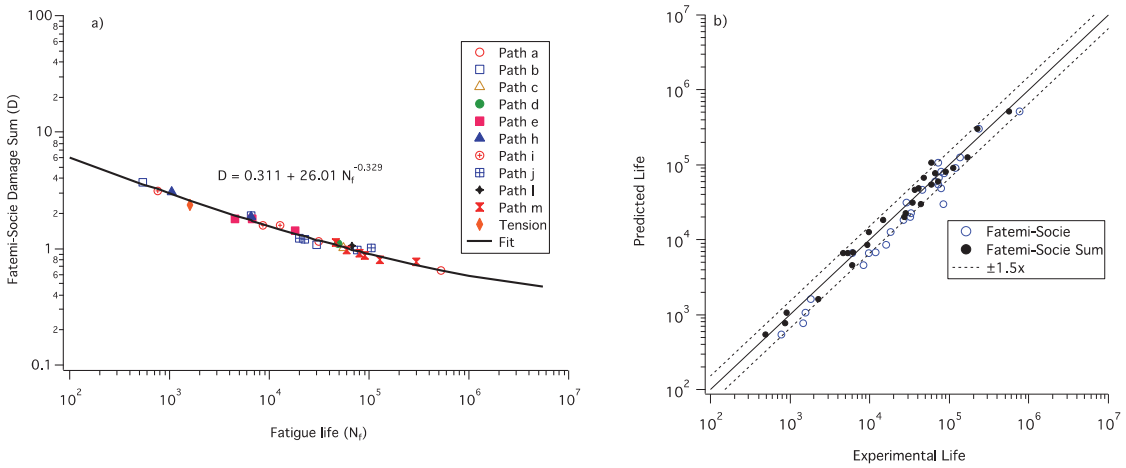

Figure 5: Fatigue damage and fatigue life prediction. a) fatigue damage and fatigue life correlation. b) Comparison between fatigue life prediction using the standard Fatemi-Socie critical plane parameter and the proposed damage summation method.

Conclusion

Parametric representation of cyclic responses from proportional and nonproportional loading was presented. These responses were successfully fitted with defined parametric equations. Similarly, Fatemi-Socie fatigue damage parameter was also represented in a parametric form. This representation shows that significant number of plans are experiencing high damage values. Therefore, it was suggested that fatigue damage shall be calculated as the sum of all incremental damage values around a stress-strain element. The proposed damage calculation technique was to improve fatigue life life prediction compared to that obtained from the critical plane method.

Acknowledgement

This research is supported by a project grant from KACST 230-34, King Abdulaziz city for science and technology, Riyadh, Saudi Arabia. The author would also like to acknowledge the support of King Fahd University of Petroleum & Minerals (KFUPM). A special thank is due to Prof. Michael Vormwald from Darmstadt University of Technology in Germany for providing the experimental data for the steel.

References

[1] Callister, W. D., Materials science and engineering: An introduction, fifth ed., J. Wiley & Sons, New York, (1999).
[2] Hertzberg, R. W., Deformation and fracture mechanics of engineering materials, fourth ed., J. Wiley & Sons, New York, (1999).
[3] Dowling, N. E., Mechanical behavior of materials: engineering methods for deformation, Fracture, and Fatigue, second ed., Prentice Hall, New Jersey, (1999).
[4] Smith, K.N., Topper, T.H., Watson, P., Stress-strain function for the fatigue of metals, J. Mater, 5 (1970) 767-778.

[5] Fatemi, A., Socie, D, A critical plane approach to multiaxial fatigue damage including out-of-phase loading, Fatigue & Fract. of Eng. Mat. & Struct., 11 (1988) 149-165.
[6] Carpinteri, A., Ronchei, C., Scorza, D., Vantadori, S., Fatigue life estimation for multiaxial low-cycle fatigue regime: The influence of the effective Poisson ratio value, Theor. Appl. Fract. Mec., 79 (2015) 77-83.
[7] Carpinteri, A., Ronchei, C., Spagnoli, A., Vantadori, S., Lifetime estimation in the low/medium-cycle regime using the Carpinteri–Spagnoli multiaxial fatigue criterion, Theor. Appl. Fract. Mec., 73 (2014) 120-127.
[8] Jiang, Y., A fatigue criterion for general multiaxial loading, Fatigue & Fract. of Eng. Mat. & Struct., 23 (2000) 19-32.
[9] Jiang, Y., Hertel, O., Vormwald, M., An experimental evaluation of three critical plane multiaxial fatigue criteria, Int. J. of Fatigue, 29 (2007) 1490-1502.
[10] Socie, D., Downing, S.D., Utagawa, S., Benchmark problems in multiaxial fatigue, Int. Conf. on Multiaxial Fat. & Fract., (2013), Koyto, Japan.
[11] Fash, J.W., Socie, D.F., McDowell, D.L., Fatigue life estimates for a simple notched component under biaxial loading, In: Miller K., Brown M., editors. Multiaxial fatigue, STP 853. ASTM, (1985) 497–513.
[12] Albinmousa, J., Jahed, H., Lambert, S., Cyclic behaviour of wrought magnesium alloy under multiaxial load, Int. J. of Fatigue, 33 (2011) 1127-1139.
[13] Albinmousa, J., Jahed, H., Multiaxial effects on LCF behaviour and fatigue failure of AZ31B magnesium extrusion, Int. J. of Fatigue, 67 (2014) 103-116.
[14] Hoffmeyer, J., Döring, R., Seeger, T., Vormwald, M., Deformation behaviour, short crack growth and fatigue lives under multiaxial nonproportional loading, Int. J. of Fatigue, 28 (2006) 508-520.
[15] Jiang, Y., Hertel, O., Vormwald, M., An experimental evaluation of three critical plane multiaxial fatigue criteria, Int. J. of Fatigue, 29 (2007) 1490-1502.